Cloud climatology at the Southern Great Plains and the layer structure, drizzle, and atmospheric modes of continental stratus

Pavlos Kollias,[1,2] George Tselioudis,[3] and Bruce A. Albrecht[4]

Received 16 March 2006; revised 7 September 2006; accepted 14 December 2006; published 15 May 2007.

[1] Long-term (6.5 years) cloud observations from the Atmospheric Radiation Measurements (ARM) program Southern Great Plains (SGP) climate research facility in Oklahoma are used to develop detailed cloud climatology. Clouds are classified with respect to their altitude (low, middle, and high), vertical development, and the presence of multilayer clouds. Single-layered cirrus, middle or low clouds were observed a total of 23% of the time the MilliMeter Cloud Radar (MMCR) was operating, and multilayer clouds were observed 20.5% of the time. Boundary layer clouds exhibit the strongest seasonal variability because of continental stratus associated with midlatitude frontal systems. Cirrus clouds are the most frequently observed cloud type and exhibit strong seasonal variability in cloud base height (higher cloud base during the summer months) and relatively constant cloud fraction. The majority of middle-level clouds are shallow with vertical extent less than 1 km. No strong seasonal cycle in the fractional coverage of multilayer clouds is observed. Continental stratus clouds exhibit strong seasonal variability with maximum occurrence during the cold seasons. Nondrizzling stratus clouds exhibit a bimodal seasonal variability with maximum occurrences in the fall and spring, while drizzling stratus occur most frequently in the winter. Thermodynamic and dynamic variables from soundings and the European Centre for Medium-Range Weather Forecasts Model (ECMWF) analyses at the SGP site illustrate an interesting coupling between strong large-scale forcing and the formation of single-layered (no other cloud layer is present) continental stratus clouds. Single-layered stratus clouds (drizzling and nondrizzling) exhibit a strong correlation with positive ω at 500 mbar and strong northerly flow.

Citation: Kollias, P., G. Tselioudis, and B. A. Albrecht (2007), Cloud climatology at the Southern Great Plains and the layer structure, drizzle, and atmospheric modes of continental stratus, *J. Geophys. Res.*, *112*, D09116, doi:10.1029/2006JD007307.

1. Introduction

[2] The representation of clouds in Global Climate Models (GCMs) remains a source of uncertainty in climate simulations. Cloud climatologies have been widely used to either evaluate climate model cloud fields or examine, in combination with other data sets, climate-scale relationships between cloud properties and dynamical or microphysical parameters. Major cloud climatologies have been based either on satellite retrievals of cloud properties [*Rossow and Schiffer*, 1999] or on surface observers' views of cloud type and amount [*Warren et al.*, 1986; *Hahn et al.*, 1994]. Such data sets provide either the top-down view of column-integrated cloud properties or the bottom-up view of the cloud field morphology. Both satellite-based and surface cloud climatologies have been successfully used to examine cloud properties, to support process studies, and to evaluate climate and weather models. However, they also present certain limitations, since the satellite cloud types are defined using radiative cloud boundaries and surface observations are based on cloud boundaries visible to human observers. As a result, these data sets do not resolve the vertical distribution of cloud layers, an issue that is important in calculating both the radiative and the hydrologic effects of the cloud field. The recently launched National Aeronautics and Space Administration (NASA) CloudSat-CALIPSO space mission, through the use of active radar-lidar observations, will help to mitigate, to a large extent, the shortcomings of passive satellite retrievals [*Stephens et al.*, 2002].

[3] Ground-based cloud radar observations resolve with good accuracy the vertical distribution of cloud layers and could be used to produce cloud type climatologies with vertical layering information [e.g., *Hogan et al.*, 2000; *Hogan and Illingworth*, 2000; *Lazarus et al.*, 2000; *Morcrette*, 2002; *Dong et al.*, 2005, 2006]. However, these observations provide point measurements only; and it is not immediately clear to what extent they are

[1]Atmospheric Science Division, Brookhaven National Laboratory, Upton, New York, USA.
[2]Now at Department of Atmospheric and Oceanic Sciences, McGill University, Montreal, Quebec, Canada.
[3]NASA Goddard Institute for Space Studies, New York, New York, USA.
[4]Division of Meteorology and Physical Oceanography, University of Miami, Miami, Florida, USA.

Copyright 2007 by the American Geophysical Union.
0148-0227/07/2006JD007307

representative of particular synoptic regimes [e.g., *Jakob et al.*, 2004]. There are different methods that can be applied to minimize this problem and to produce cloud layering climatologies useful for both cloud process and model evaluation studies. If a radar system is run continuously over a number of years, it eventually samples a large number of dynamical and microphysical regimes. If additional data sets are used to put the cloud layering information into the context of large-scale or mesoscale dynamical regimes, such information can be used to study interactions among cloud vertical distributions and dynamical and microphysical processes and to evaluate the ability of models to simulate those interactions.

[4] Because of their large horizontal extents and high reflectivity, midlatitude storm systems impact on Earth's net radiation budget is larger than any other cloud regime [*Harrison et al.*, 1990]. Cloud radiative forcing in the midlatitudes is strongly tied to the dynamics of baroclinic storm systems. *Tselioudis et al.* [2000] found that differences in net radiative fluxes between low- and high-pressure regimes in the northern midlatitudes introduce a wintertime warming in the low- versus the high-pressure regimes of 5–15 W m^{-2} and a cooling in all other seasons of 10–40 W m^{-2}. This cloud radiative forcing is not well represented in climate models because of large errors in their simulations of midlatitude clouds and subsequently their radiation effects [*Norris and Weaver*, 2001; *Tselioudis and Jakob*, 2002]. A better understanding between the linkages of cloud types and atmospheric dynamics could help to improve the representation of midlatitude cloud variability in numerical models.

[5] Despite major research efforts on marine stratocumulus, relatively little work has focused on continental midlatitude stratus and stratocumulus clouds [*Del Genio et al.*, 1996; *Del Genio and Wolf*, 2000; *Dong et al.*, 2000]. Even though midlatitude continental clouds directly affect a relatively small area of the Earth's surface compared with their marine counterparts, they affect local climate and weather and are linked closely to surface temperature and water budgets as well as diurnal cycles [e.g., *Sassen et al.*, 1999; *Kollias and Albrecht*, 2000; *Dong et al.*, 2005, 2006]. Changes in cloudiness or other properties of continental clouds may, in fact, explain a substantial portion of the observed increase in global temperatures during the last century due to a decrease in the diurnal range of surface temperatures over the continents [e.g., *Ramanathan et al.*, 1989; *Cess et al.*, 1990; *Karl et al.*, 1993]. *Tselioudis and Jakob* [2002] evaluate a weather forecast (ECMWF) and a climate (GISS) model using satellite observations and find that both models severely underestimate midlatitude continental cloud amounts and overestimate their optical depths.

[6] The U.S. Department of Energy's Atmospheric Radiation Measurement (ARM) program has established several Climate Research Facilities (ACRF) that provide continuous, long-term observations of clouds and radiation [*Ackerman and Stokes*, 2003]. ARM, with its overall goal of improving the treatment of radiation and clouds in climate models [*Stokes and Schwartz*, 1994], has provided unique observing systems for accelerating progress on the parameterization of cloud processes. Six and a half years (January 1998 to June 2004) of cloud observations collected at the Southern Great Plains (SGP) ACRF are used to produce the cloud-type climatology. The climatology provides cloud amounts for seven different cloud types as well as information on the detailed structure of multilayer cloud occurrences. Furthermore, the European Centre for Medium-Range Weather Forecasts (ECMWF) hourly averaged model output defines the dynamic regimes present during the observations of the cloud conditions by the vertically pointing active remote sensors at the SGP ACRF. The cloud-type climatology and the ECMWF SGP data set are then analyzed to examine and map dynamical conditions that favor the creation of single-layer versus multilayer cloud structures as well as dynamical conditions that favor the occurrence of drizzle in continental stratus clouds.

2. ARSCL-Based Cloud Climatology

[7] Ground-based active remote sensors such as the Millimeter-wavelength Clouds Radars (MMCR [*Moran et al.*, 1998]) have distinct advantages over passive satellite measurements when it comes to cloud profiling, especially in multilayer cloud scenes. MMCRs can provide detailed, high-resolution measurements of cloud boundaries and reflectivity that can penetrate multilayer clouds, and thus provide detailed cloud layer overlap information. The basic data set used in this study is the Active Remote Sensing Cloud Locations product (ARSCL [*Clothiaux et al.*, 2000]), which combines MMCR, ceilometer and MicroPulse Lidar (MPL) observations, and provides the most accurate representation of clouds above the SGP ACRF with a temporal resolution of 10 s and vertical resolution of 45 m [e.g., *Clothiaux et al.*, 2000; *Kollias et al.*, 2005].

[8] Profiles of MMCR radar reflectivity obtained every 10 s are used to produce hourly estimates of cloud fraction, base, top and thickness for each cloud type and enable the detection of multilayer cloud scenes. Clouds are objectively classified according to their vertical extent; cloud base height, and the presence or not of precipitation (Figure 1). If the MMCR echo base [*Clothiaux et al.*, 2000] extends in the lowest 200 m above the ground, the cloud is classified as precipitating. Depending on their cloud top height, precipitating clouds are classified into precipitating shallow clouds with cloud tops below 2 km, and deep precipitating clouds with cloud tops above 2 km. In addition to low cloud base, a minimum reflectivity criterion in the column (−15 dBZ) is required for the identification of precipitating clouds (shallow or deep). This eliminates the misclassification of very low cloud base stratus clouds or fog as precipitating cloud. Deep precipitating clouds are further classified with respect their precipitation intensity. Unexpectedly, there were no surface-based quantitative measurements of precipitation (e.g., rainfall rate) at the ARM SGP site during the observing period. Only recently (2006), a disdrometer was added in the instrument list at the ARM SGP site to provide quantitative measurement of raindrop size distributions and rainfall intensity. In addition, the MMCR receiver saturated in the presence of light to moderate rainfall rates (higher than 1–2 mm h^{-1}) and thus MMCR radar reflectivity cannot be used as a measure of rainfall intensity. We decided to use the microwave radiometer wet window flag as a qualitative indicator of precipitation intensity. If the microwave radiometer (located near the MMCR) precipitation sensor detects the presence of water on the mirror of the

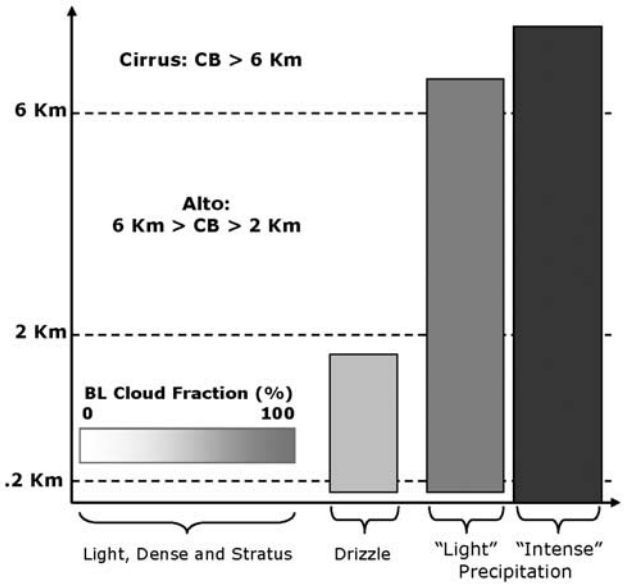

Figure 1. Schematic representation of the cloud classification applied to the ARSCL data set.

sensor, then the deep precipitating clouds is classified as "intense," otherwise is classified as low-rainfall rate precipitating cloud ("weak"). The microwave radiometer wet window flag is conveniently included as a variable in the ARSCL files. Precipitation in the form of virga from clouds with radar echoes that do not reach near the ground are not considered as precipitating.

[9] Nonprecipitating clouds are classified into the following categories: (1) nonprecipitating BL clouds when the cloud base is above 0.2 km and the cloud top below 2 km, (2) deep BL clouds when the cloud base is between 0.2 and 2 km and the cloud top is higher than 2 km, (3) middle clouds when the cloud base is between 2 and 6 km and (4) cirrus clouds if the cloud base is above 6 km. BL clouds are further classified according to their hourly averaged fractional coverage (FC) to: "stratus" if their hourly averaged FC is larger than 80%, "dense cu" if their hourly averaged FC is less than 80% and larger than 30% and "light cu" if their hourly averaged FC is less than 30%. These three classes are calculated for both drizzling and nondrizzling BL clouds. The addition of BL cloud subcategories with respect to their hourly averaged FC is necessary for the identification and study of continental stratus clouds. The threshold FC values selected for these three classes are qualitatively established and provide only broad classifications. The identified cloud types are further classified into two groups: periods when a particular cloud type (e.g., cirrus, middle and BL) is the only layer observed at the SGP site (single layer) and periods when two or more cloud types are present (multilayer cloud scenes). Single-layered cloud periods such as postfrontal continental stratus clouds are often associated with strong large-scale forcing such as subsidence and cold advection, while the multilayer cloud scenes require a complex profile of large-scale forcing or include long-lived, residual cloud products. Although observed at vertical incidence, the long record of the vertical structure of cloudiness over the ARM SGP, the amount of single-layer and multilayer cloud periods and its seasonal variability can be compared with satellite derived cloud products and climatology (e.g., International Satellite Cloud Climatology Project (ISCCP) [*Rossow and Schiffer*, 1999]) and model output (e.g., ECMWF). Additional products of the cloud climatology include hourly estimates of cloud base and –top heights and cloud thickness for various cloud types and boundary layer wind speed, direction, and static stability obtained from atmospheric soundings.

[10] In addition to the ARSCL observations, the ECMWF hourly averaged model output centered on the ARM-SGP site (Lon: 261.7–263.0°E, Lat: 36.0–37.0°N) for the same period is analyzed. The model output is compared with cloud conditions observed by the vertically pointing active remote sensors at the SGP. An assessment of the ECMWF model cloudiness (all cloud types) compared with the ARSCL-based cloud climatology will be the focus of future work, although short-term assessment of the ECMWF model cloudiness has been conducted in the past using ARM observations [e.g., *Morcrette*, 2002]. In this study, the focus is on the observed cloud climatology and the relationship between the observed macroscopic properties of boundary layer clouds and the ECMWF model predicted and diagnosed dynamical parameters.

3. Cloud Climatology at the ARM SGP

[11] The MMCR operates continuously at the SGP since 1996 and its excellent operational integrity and stability provides the basis for a multiyear cloud and precipitation record. The cloud and precipitation climatology presented here is derived from time periods when the MMCR was in good operating status (84% of the time within the 6.5 years period). The MMCR cycles over several operational modes [*Clothiaux et al.*, 2000; *Kollias et al.*, 2005], and thus maximizes sensitivity for various cloud types. The MMCRs, together with the MPL are the primary observing tools for quantifying the properties of nearly all radiatively important clouds over the ARM sites. This includes a wide range of cloud types, from shallow fair weather cumuli and stratus in the boundary layer to thin cirrus and convective anvils in the upper troposphere.

3.1. Cloud Fraction per Cloud Type

[12] Figure 2a shows the monthly averaged FC of deep precipitation over the SGP site for the period January 1998 to June 2004. Deep precipitation exhibits a moderate seasonal variability with a maximum (7.7%, see Table 1) during the November-March period (NDJFM) and a minimum (4.6%) in the summer months June-August (JJA). Long-lived deep precipitation associated with the passage of midlatitude cyclones and frontal systems could explain the maximum FC in NDJFM and the large fraction of weak precipitation. During JJA, isolated convective clouds are often observed. This could explain the small monthly averaged FC of deep precipitation at SGP and the relatively large fraction of intense deep precipitating conditions (higher reflectivities and surface rainfall rate). The variability of the fractional coverage for all types of clouds at the SGP site during the cold (NDJFM), warm (JJA) and annual period is summarized in Table 1.

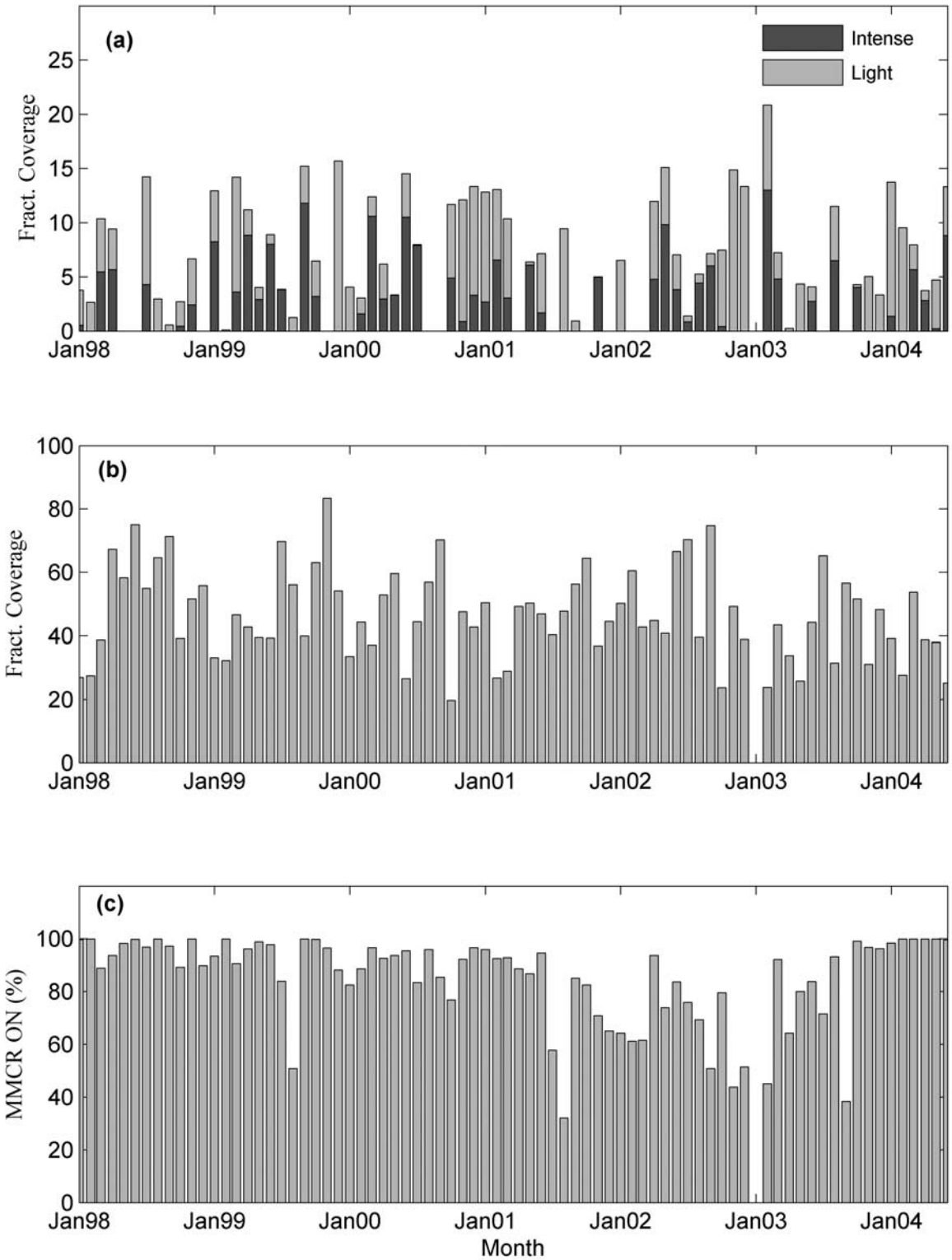

Figure 2. Monthly averaged fractional coverage of (a) deep precipitating clouds, (b) clear skies and (c) MMCR operational time.

Table 1. Annual, Winter (NDJFM), and Summer (JJA) Cloud Climatology at the ARM SGP Site for the Period January 1998 to June 2004 Derived From the ARSCL Database[a]

Cloud Type	Fractional Coverage (NDJFM), %	Fractional Coverage (JJA), %	Fractional Coverage (Annual), %
Cirrus	29.7	30.3	28.9
Single cirrus	15.4	14.4	14.1
BLC	23.5	10.8	18.6
Single BLC	8.0	2.3	5.7
Middle	18.6	15.5	17.2
Single middle	3.3	3.1	3.1
Total single	26.2	19.8	22.9
Precipitation	7.7	4.6	6.1
BLC and cirrus	4.5	3.4	4.1
BLC and middle	3.8	2.2	3.3
Cirrus and middle	6.9	8.5	7.1
BLC, middle, and cirrus	5.8	5.2	5.6
Multilayer (B, M, C)	21.0	18.3	20.1
Multilayer (PR, other)	6.1	4.0	5.3
Clear sky	40.0	52.9	46.0

[a]B, low clouds; M, middle clouds; C, cirrus clouds; PR, precipitation. The multilayer (B, M, C) category corresponds to the total fractional coverage of multilayer scenes that contain in the same 1-hour period a combination of B, M and C cloud types. The multilayer (PR, other) category corresponds to the total fractional coverage of multilayer scenes that contain in the same 1-hour period PR and one other cloud type (B, M, C) observations. The seasonal and annual averages are based on hourly estimates of fractional coverage for each cloud type. When multilayer conditions were observed in the same 1-hour period, the fractional coverage of the layer with the higher 1-hour fractional coverage was used as estimated multilayer 1-hour fractional coverage. This definition is consistent with the clear sky definition. The presented cloud and precipitation climatology is derived only from time periods that the MMCR was in good operating status (84% of the time) and not a total of 6.5 years.

[13] The monthly averaged FC clear skies and the time the MMCR was in good operational status are also shown in Figure 2b. Clear skies are more often observed in JJA (52.9%) and less in NDJFM (40.0%). The clear sky fraction seasonal variability also reflects the difference in large-scale atmospheric dynamics between the summer and the winter and transition periods at the SGP. Clear skies and deep precipitation (excluding precipitating BL clouds) account for more that half (52.1%) of the total MMCR observations at the SGP site during the 1998–2004 period. The residual is distributed among three main cloud types: low or BL clouds, middle clouds and cirrus clouds.

[14] The monthly averaged FC of cirrus, middle and BL clouds is shown in Figure 3. Cirrus clouds have the highest annual FC (29%). Although the cold and warm season averaged FC shows small variability, a month-by-month analysis indicates that the minimum cirrus FC is observed in September (16%), the maximum in June (37%) and a secondary winter maximum in observed in January (33%). Middle level clouds exhibit a weak seasonal cycle (Table 1) with 20% FC in NJDFM and 15% in JJA. In contrast, BL clouds exhibit strong seasonal variability with a minimum FC observed during the summer months (10%) and over 23% during the NDJFM period. The BL clouds FC distribution during the cold season exhibits a bimodal structure with a maximum FC during October–November and March–April and a local minimum in January. Drizzling BL clouds are mostly observed during the cold season, associated with prefrontal and postfrontal BL stratus clouds. During the warm season, broken BL clouds (fair weather cumuli) are responsible for the low FC.

3.2. Single-Layer and Multilayer Cloud Scenes

[15] The main cloud layer types (cirrus, middle and BL) are further classified as single-layer (SL) and multilayer (ML) cloud scenes. If during the 1-hour interval of ARSCL observations, used as our fundamental cloud climatology unit, only one particular cloud type is observed, then this 1-hour period is classified as a SL cloud period. A minimum of 5% hourly averaged FC of a particular cloud type is required for an observed 1-hour period to be classified as a SL cloud type. If more than one cloud type is observed during the same 1-hour observation period, then the cloud scene is classified as ML. Thus ML cloud scenes are classified with two cloud types (e.g., BL-cirrus, BL-middle, cirrus-middle) and three cloud types (BL-middle-cirrus) simultaneously present during the 1-hour observing period. The same minimum 5% hourly averaged FC for each cloud type involved in the ML cloud scene is required. The ML cloud scene hourly averaged FC is equal to the FC of the cloud layer with the maximum FC. In addition to the ML cloud scenes based on combinations of cirrus, middle and BL clouds, we define another type of ML cloud scene that combines precipitation (PR) and another cloud type (e.g., cirrus). The 5% minimum hourly averaged FC per cloud type generates a small cloudiness residual, since cloud scenes with less than 5% FC are not presented in the single-layered and multilayered statistics in Table 1. Thus the sum of total single-layered and multilayered scenes, precipitation and clear skies is not necessarily equal to 100%.

[16] The climatology of SL and ML cloud scenes could improve our understanding on how atmospheric dynamics affect cloudiness. This is based on the hypothesis that large-scale atmospheric forcing correlates better with cloud types than cloud fraction. The existence of SL and ML cloud scenes also affects satellite-based retrievals of cloud top height and microphysics. The seasonal variability of SL boundary layer, middle and cirrus clouds is shown in Figure 4. Overall, SL cloud conditions are observed 23% of the time, with a maximum FC in NDJFM (26%) and a minimum in JJA (20%, Table 1). Nearly half of observed cirrus clouds are SL cirrus clouds that have weak seasonal cycle except for a dip in September. SL middle clouds show almost no seasonal variability and are only a small fraction (3%) of the overall middle cloud FC (17%) indicating that middle level clouds are often associated with the presence of other cloud types and especially cirrus clouds (Table 1).

[17] Boundary layer, cirrus and middle clouds coexist in the same 1-hour period in ML cloud scenes (any combination of two cloud types or all three) 20.1% of the time. Deep precipitating clouds and another cloud type in the same hour are observed 5.3% of the time. Thus, in total 25.4% of the 1-hour periods that the MMCR was operational we observed ML cloud scenes. The most commonly observed ML cloud scene is cirrus-middle with a maximum (8.5%) in JJA when cloud deentrainment from summer thunderstorms can inject cloud mass at various levels (Figure 4).

3.3. Cloud Layer Base and Thickness

[18] Hourly averaged cloud layer base and thickness estimates are used to construct composite frequency of occurrence distributions. Figure 5 shows the frequency of

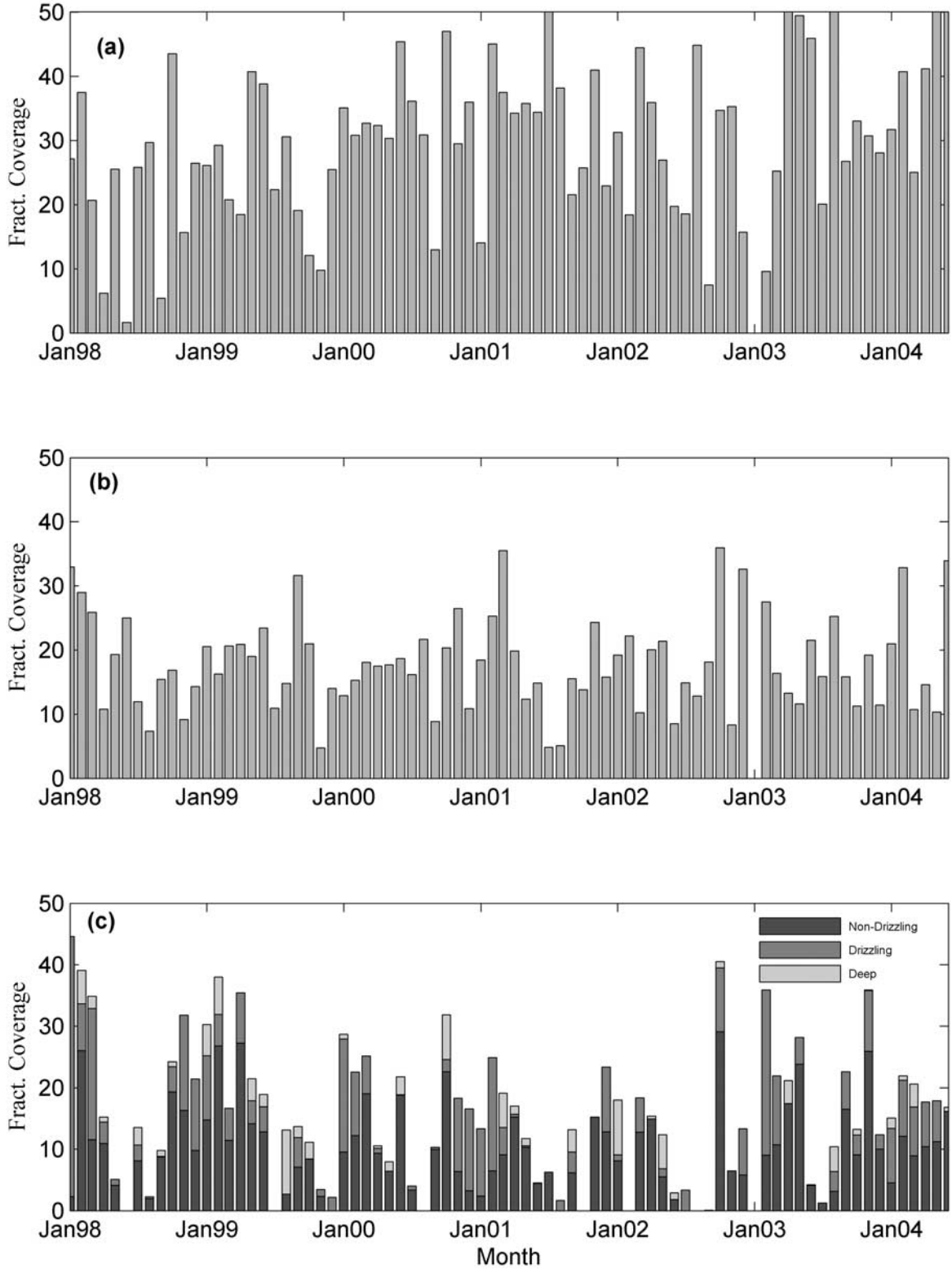

Figure 3. Monthly averaged fractional coverage of (a) cirrus clouds, (b) middle clouds and (c) boundary layer clouds. The boundary layer clouds (Figure 3c) are also classified in nondrizzling, drizzling and deep categories according to the ARSCL-based classification.

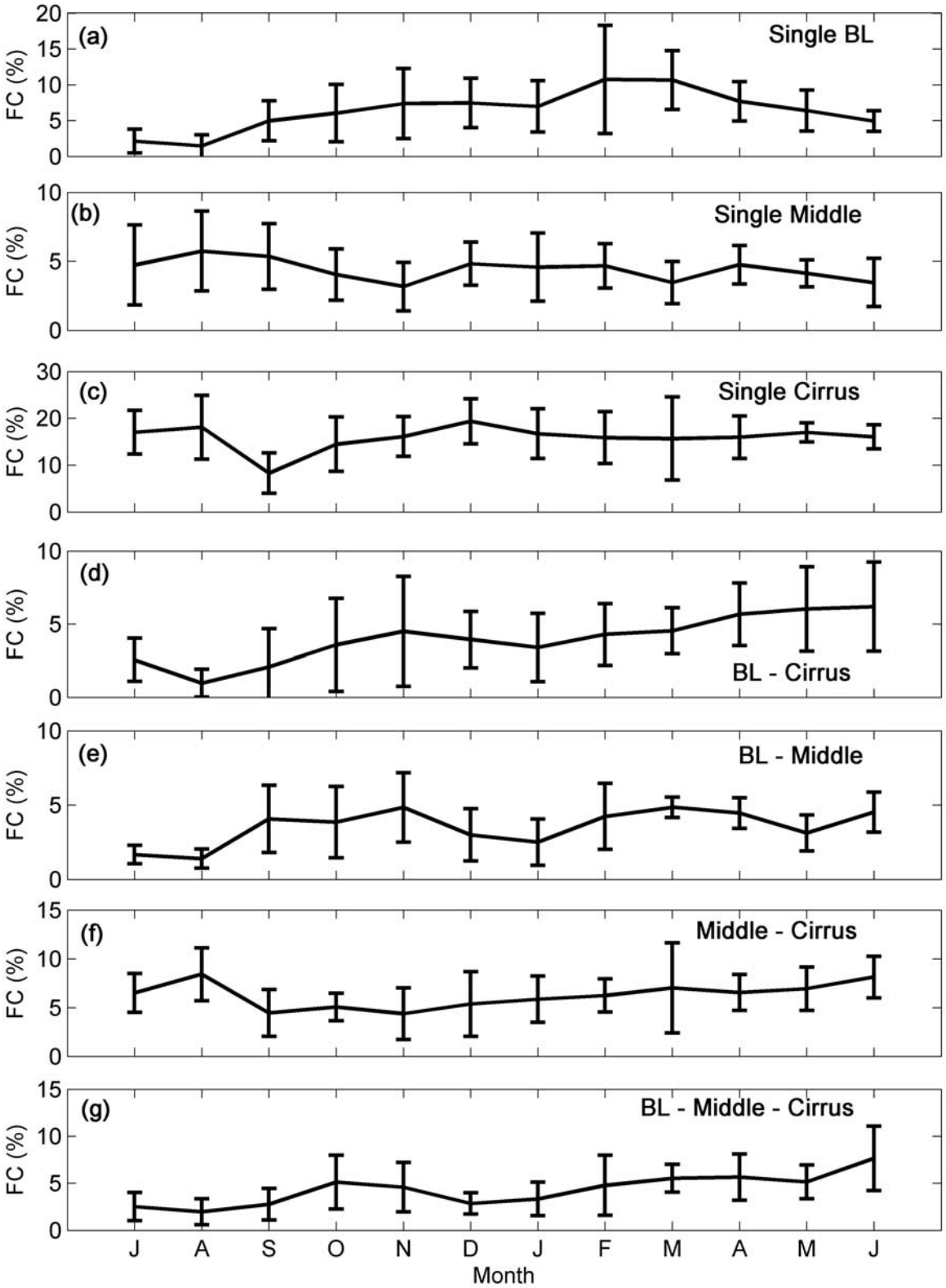

Figure 4. Seasonal variability of single-layer clouds scenes (no over cloud layer is present) of (a) BL clouds, (b) middle clouds and (c) cirrus clouds from 1998 to 2004 and associated error bars (one standard deviation on the monthly averaged values). Monthly averaged fractional coverage and associated error bars of multilayer cloud scenes: (d) BL-cirrus, (e) BL-middle, (f) middle-cirrus and (g) BL-middle-cirrus.

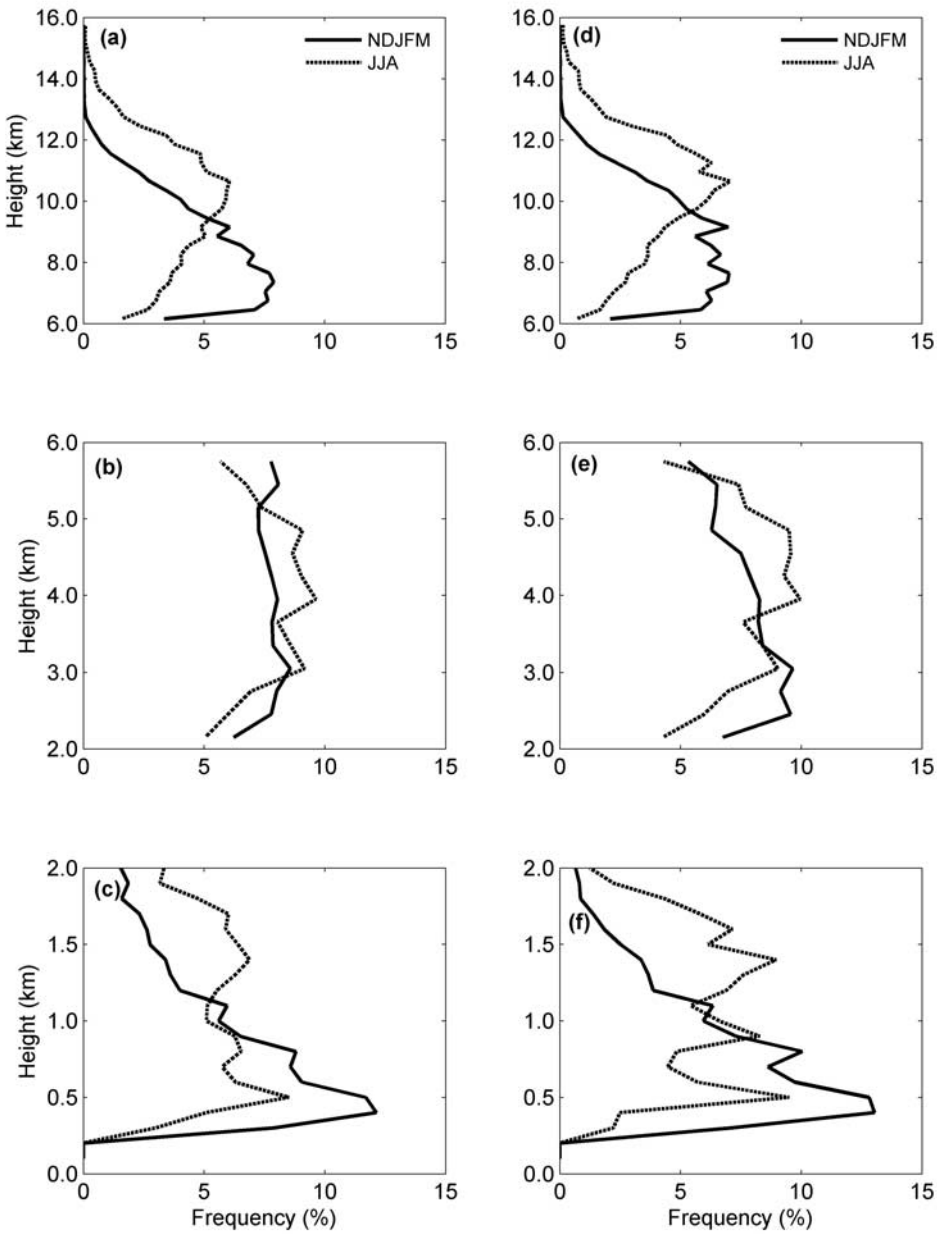

Figure 5. Frequency of occurrence of cloud base for (a) cirrus, (b) middle and (c) BL clouds for NDJFM (solid) and JJA (dashed) when all cloud layer occurrences (single-layer and multilayer) are considered. Frequency of occurrence of cloud base for (d) cirrus, (e) middle and (f) BL clouds for NDJFM (solid) and JJA (dashed) during single-layer conditions only.

occurrence of cloud base for cirrus, middle and BL clouds for NDJFM and JJA during SL and ML only cloud scenes. Cirrus clouds have lower cloud bases during the cold season when the cloud base distribution peaks at 7.8 km, while the cloud bases are higher during the summer months (peak at 10.2 km). SL cirrus clouds exhibit a bimodal cloud base distribution during the cold season. Middle clouds have a uniform distribution of cloud bases (3–6 km) during the cold season and a 4.2 km peak in the cloud base distribution during the summer season. SL middle clouds exhibit a pronounced cloud base peak at 2.8 km during in NDJFM and a bimodal cloud base distribution during JJA. The cloud base distribution of BL clouds has a strong peak at 0.5 km in NDJFM and a trimodal cloud base distribution with higher cloud bases in JJA. The trimodal BL cloud base distribution in JJA is more pronounced in SL boundary layer clouds. This suggests that SL boundary layer clouds are responsible for the trimodal cloud base signature when all boundary layer clouds are considered. In general, the partitioning of the cloud types to SL and ML indicates the

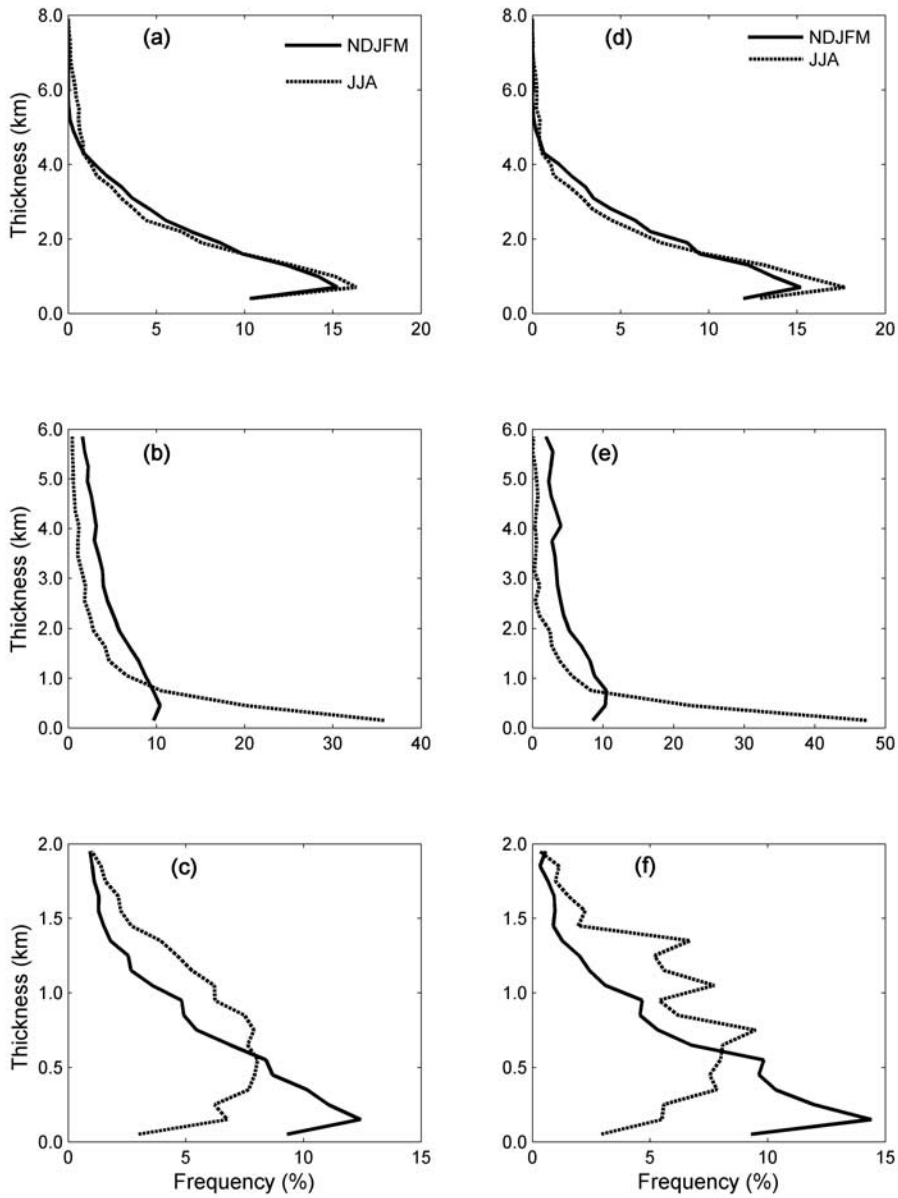

Figure 6. Frequency of occurrence of cloud thickness for (a) cirrus, (b) middle and (c) BL clouds for NDJFM (solid) and JJA (dashed) when all cloud layer occurrences (single-layer and multilayer) are considered. Frequency of occurrence of cloud thickness for (d) cirrus, (e) middle and (f) BL clouds for NDJFM (solid) and JJA (dashed) during single-layer conditions only.

presence of multimodal cloud base distributions when SL cloud scenes are only considered.

[19] Figure 6 shows the cloud thickness distribution of cirrus, middle and BL clouds for NDJFM and JJA seasons and for SL and ML cloud scenes. Cirrus clouds exhibit remarkably similar cloud thickness distributions for both seasons and cloud scene types. The majority of the cirrus clouds have cloud thickness less than 2 km, and the cloud thickness distribution peaks at 1 km. More than 20% of cirrus clouds are thin with cloud thickness less than 0.8 km. In contrast, the cloud thickness distribution of middle clouds exhibit great seasonal variability. During the cold season, the cloud thickness of middle clouds peaks at 1 km and gradually decreases with altitude. During the summer months, a large percentage of middle clouds (30% for all middle clouds, 50% for SL middle clouds) have cloud thickness less than 300 m. SL middle clouds are rarely more than 2 km thick. The seasonal variability of middle cloud could have significant affect on satellite retrievals. The cloud thickness distribution of BL clouds also exhibits strong seasonal variability. During the summer months, BL clouds (both SL and ML cloud scenes) have typical cloud thickness between 0.5 and 1.0 km. BL clouds are shallower during the cold season, when the cloud thickness distribution peaks at 0.2–0.3 km. The difference in the cloud thickness of BL clouds during the warm and cold season

Table 2. Annual, Winter (NDJFM), and Summer (JJA) Climatology of BL Clouds at the ARM SGP Site for the Period January 1998 to June 2004 Derived From the ARSCL Database[a]

BL Cloud Type	Cloud Scene	Drizzle Amount	Fraction of 1-Hour Periods (NDJFM), %	Fraction of 1-Hour Periods (JJA), %	Fraction of 1-Hour Periods (Annual), %
"Stratus"	all	all	18.7	4.8	13.1
"Dense Cu"	all	all	6.3	7.2	7.1
"Light Cu"	all	all	6.5	12.4	9.3
"Stratus"	ML	NO	5.7	3.1	5.2
"Stratus"	SL	NO	2.9	0.8	2.5
"Stratus"	ML	yes	5.0	0.2	2.6
"Stratus"	SL	yes	2.8	0.1	1.3

[a]Fractional coverage categories: Stratus, FC > 80%; Dense Cu, 80% > FC > 30%; Light Cu, CF < 30%. Cloud scene categories: all, both single-layer and multilayer cloud scenes; ML, multilayer cloud scene; SL, single-layer cloud scene. Drizzle amount category: all, both drizzling and nondrizzling BL clouds; NO, nondrizzling stratus; yes, drizzling stratus. The presented cloud and precipitation climatology is derived only from time periods that the MMCR was in good operating status (84% of the time) and not a total of 6.5 years.

is attributed to the presence of stratus clouds during the winter and fair weather cumuli during the summer. The BL cloud climatology is the subject of the following section.

4. BL Cloud Climatology at the ARM SGP

[20] Boundary layer clouds and continental stratus in particular, exhibit the largest seasonal variability [e.g., *Dong et al.*, 2000, 2005, 2006; *Mace et al.*, 2001]. Their large seasonal variability indicates possible coupling mechanisms between the continental stratus clouds formation and the large-scale dynamics that also exhibit great seasonal variability at midlatitudes. Before we investigate this relationship between the large-scale forcing and continental stratus, a more detailed climatology of BL clouds is presented. A factor that limits the radar-based only detection of BL clouds during the warm season is the presence of high concentrations of bugs and insects in the lowest 2–3 km. This results in strong noncloud radar returns (clutter) and thus makes the MMCR-based BL cloud detection difficult. However, the combination of active sensors (MPL, ceilometer and MMCR) in ARSCL [*Clothiaux et al.*, 2000] substantially improves our ability to detect the BL cloud boundaries.

[21] BL clouds are classified with respect to their hourly averaged fractional coverage as "stratus," "dense cu" or "light cu." These cloud scenes have different cloud fractional coverage. We treat the occurrence of one of

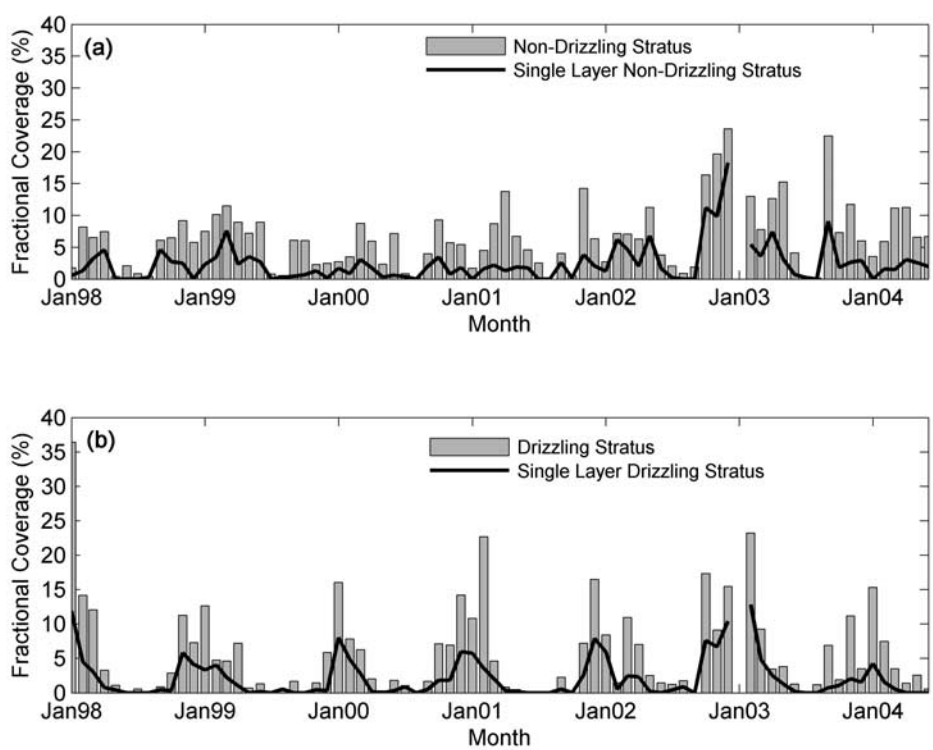

Figure 7. Monthly averaged fractional coverage of (a) nondrizzling stratus clouds (bars) and single-layer (no over overlapping layer) nondrizzling stratus (black line) observations and (b) drizzling stratus clouds (bars) and single-layer (no over overlapping layer) drizzling stratus (black line) observations.

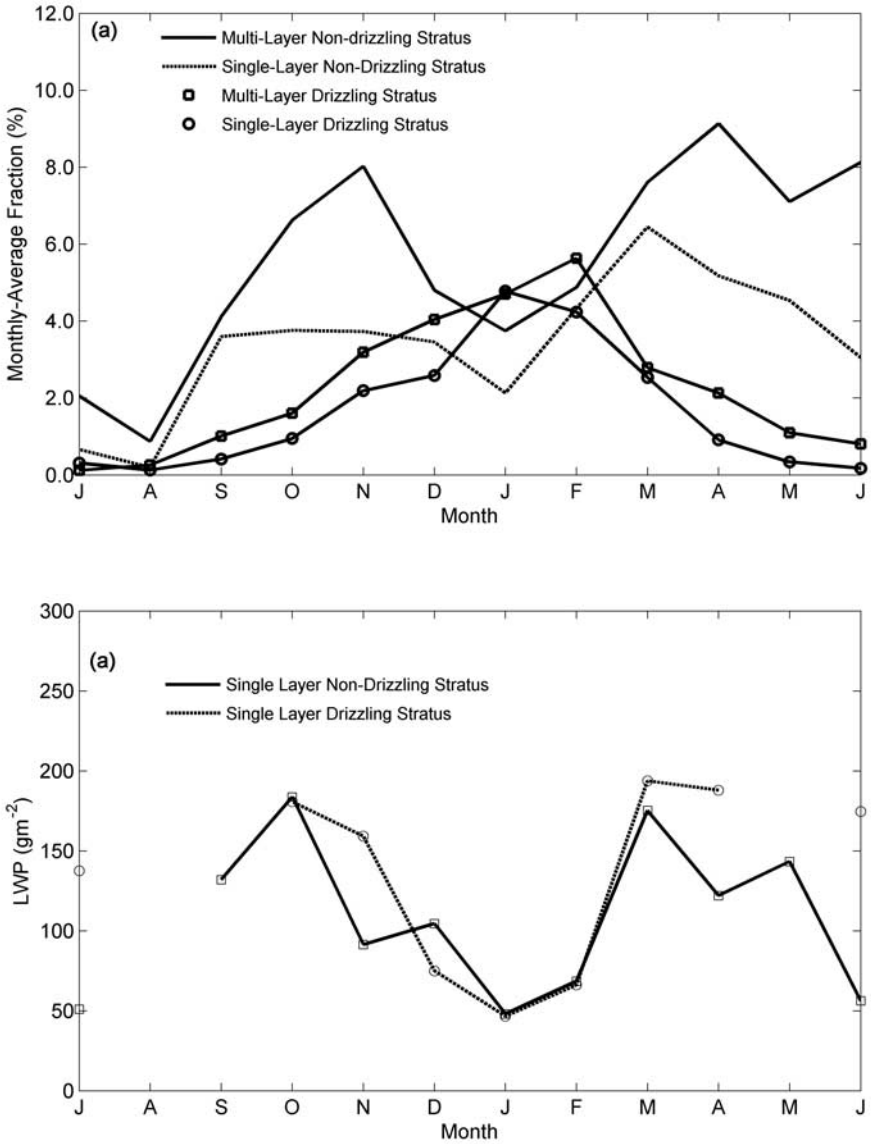

Figure 8. Seasonal variability of (a) fractional coverage for the four stratus cloud subcategories and (b) LWP during single-layer stratus cloud conditions.

these three different cloud types as an event and we calculate the frequency of occurrence of these events per cloud scene (Table 2). This approach removes the actual cloud fraction from the analysis and allows us to focus on the climatology of cloud scenes rather than cloud fraction. In addition, BL clouds are classified according to the amount of drizzle and cloud scene type (SL or ML). It is emphasized that the numbers shown in Table 2 correspond to fraction (%) of 1-hour periods that a particular BL cloud type occurred (at zenith viewing) without considering the absolute fractional coverage of these BL cloud types. Stratus clouds scenes have the strongest seasonal variability from all BL cloud scenes with maximum occurrence (18.7%) in NDJFM and minimum (4.8%) in JJA where stratus clouds are rarely observed. Broken BL cloud scenes have their maximum occurrence in JJA; the only season of the year when the frequency of occurrence of broken BL cloud scenes exceeds the frequency of occurrence of stratus BL clouds (Table 2).

[22] Continental stratus (hourly averaged cloud fraction >80%) cloud scenes are further classified into four subgroups according to their drizzle amount. We are only interested in the extreme presence or absence of drizzle within the 1-hour observations and define a stratus scene as drizzling if drizzle is observed more than 80% of the time, and a stratus scene as nondrizzling if no amount of drizzle is observed. In addition we subgroup the scenes in ML or SL groups. Figure 7 shows the monthly averaged fractional coverage of these four continental stratus groups during our observing period. The black line shows the monthly averaged fractional coverage of SL stratus and the bars the total (SL and ML) monthly averaged fractional coverage of stratus clouds. Drizzling stratus cloud con-

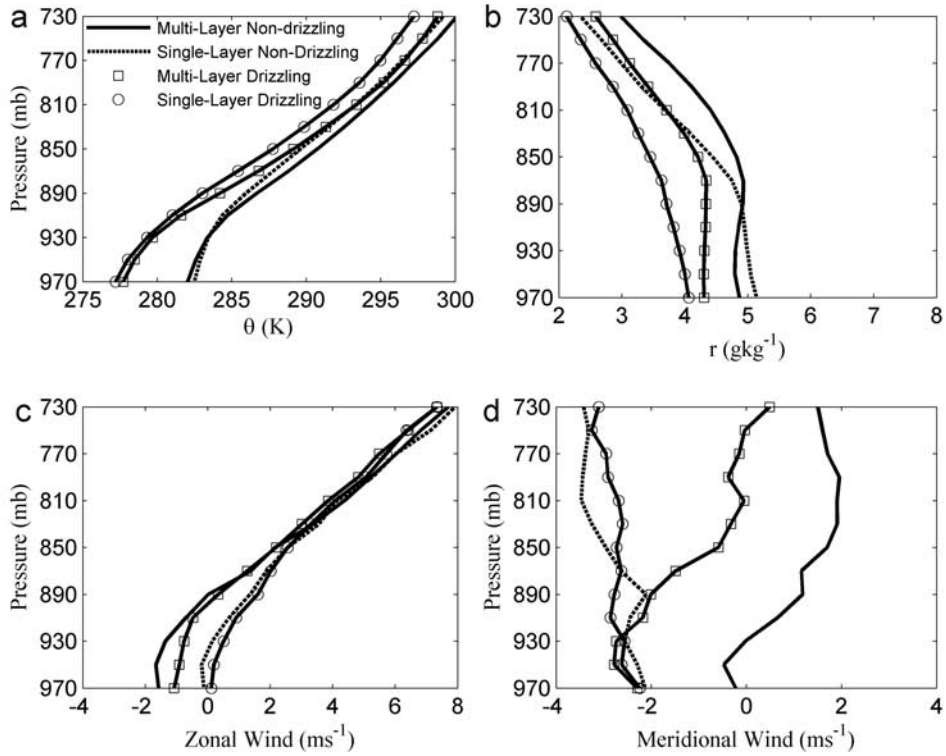

Figure 9. First principal component mode of (a) potential temperature ϑ (K), (b) mixing ratio r (g kg^{-1}), (c) zonal wind component (m s^{-1}), and (d) meridional wind component (m s^{-1}).

ditions (in either ML or SL cloud scenes) are rarely observed during the summer months (Table 2). Nondrizzling stratus clouds, when observed during the summer months, are usually part of multi layer cloud scenes. The highest fraction of hours of the month with stratus cloud is observed during the cold season. The seasonal variability of all (ML and SL) and SL stratus clouds for drizzling and nondrizzling conditions (Figure 8a) reveals a bimodal distribution with maximum fractional coverage during November and March and a local cold season minimum in January not found previously [*Dong et al.*, 2005, 2006]. In contrast, the seasonal distribution of drizzling stratus clouds peaks in January (Figure 8). The seasonal distribution of Liquid Water Path (LWP) during SL cloud scenes is shown in Figure 8. The LWP seasonal distribution reveals a bimodal structure that peaks during the all-cloud-scenes (SL and ML) maxima in November and March. The peak in precipitating stratus occurs during the minimum in the LWP distribution. It is possible, however, that low temperatures (below 0°C) during the coldest months and the phase change from liquid to ice decrease the monthly averaged LWP compared with warmer clouds and enhance the precipitation efficiency of stratus clouds during this time.

5. Continental Stratus, Thermodynamics Structure, and Subsidence

[23] Using the detailed continental stratus climatology presented in the previous section, we investigate the coupling between the mean thermodynamic structure and midlevel (500 mbar) stability and the formation of continental stratus during the cold season. Initially, time periods where the four continental stratus subcategories (ML nondrizzling, SL nondrizzling, ML drizzling and SL drizzling) are observed at the ARM SGP site are identified. Furthermore, only cases with at least 3 consecutive hours of the same stratus cloud conditions are used. The ECMWF model output is used to estimate the thermodynamic structure (potential temperature (θ), mixing ratio (r), zonal (U) and meridional (V) wind and midlevel (500 mbar) vertical velocity (ω) for the time periods that correspond to the four continental stratus subcategories. The model outputs are averaged hourly over a large grid box around the ARM SGP site (Lon: 261.7–263.0, Lat: 36.0–37.0). The use of the ECMWF model hourly output is used to estimate the thermodynamic structure and stability of the atmosphere near the SGP site during periods with no sounding launch.

[24] On the basis of the cloud classification, soundings (3–4 per day) launched when one of the four continental stratus cloud types was observed at the ARM SGP are identified. The soundings were further grouped into four categories that correspond to the respective continental stratus subcategories. Principal component analysis (PCA) is used to identify the dominant atmospheric thermodynamic modes that explain most of the observed variance in the soundings for each cloud type [e.g., *Zivkovic and Louis*, 1992; *Gottschalck et al.*, 2000]. The number of soundings per stratus clouds subcategory available for the PCA varied from 200 to 330 and were all selected during the NDJFM cold season only. The PCA input array consists of an atmospheric profile with 52 components: 13 levels of

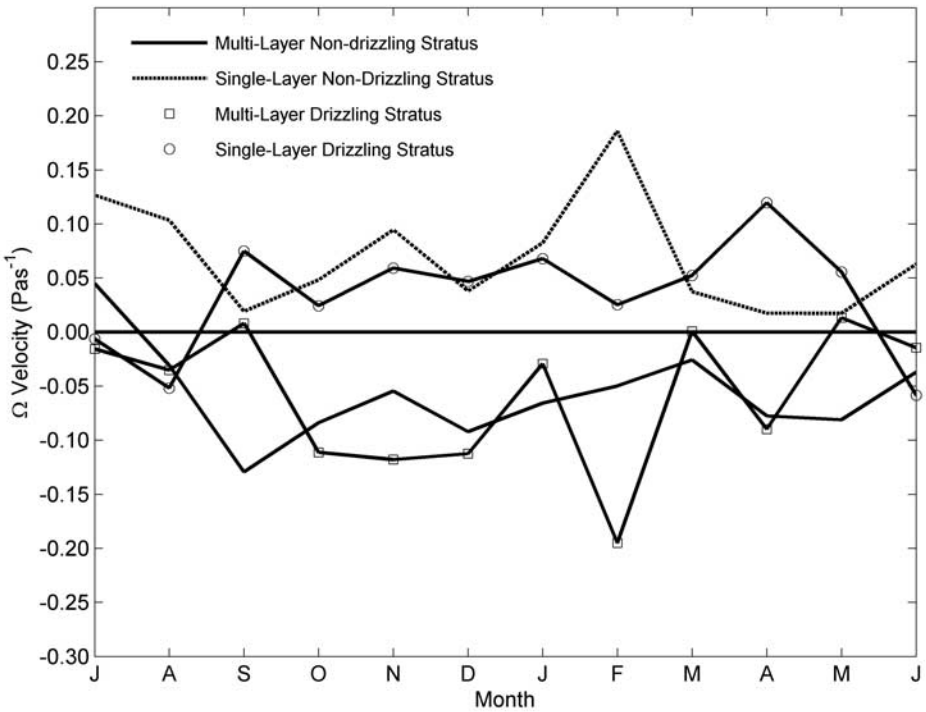

Figure 10. Seasonal variability of ECMWF ω velocity (Pas^{-1}) at 500 mbar over the 1998–2004 period for the four stratus clouds cases: multilayer nondrizzling stratus clouds (solid), multilayer drizzling stratus clouds (square), single-layer nondrizzling, stratus clouds (dashed) and single-layer drizzling stratus clouds (circles).

potential temperature (θ), mixing ratio (r), zonal wind (U), and meridional wind (V). The pressure levels are from 970 to 720 mbar, spaced every 20 mbar. The atmospheric profiles from each stratus type group were input to the PCA and the principal modes for the four atmospheric variables (θ, r, U and V) were extracted.

[25] Figure 9 shows the first PCA mode of the potential temperature, mixing ratio, zonal and meridional wind (explains 49–58% of the observed variance in the soundings) for all four continental stratus cloud categories. The potential temperature and mixing ratio first PCA mode profiles (Figures 9a and 9b) group favorable conditions for the generation of drizzling versus nondrizzling cloud structures. The wind-component first PCA mode profiles (Figures 9c and 9d) group favorable conditions for the occurrence of multilayer versus single-layer cloud structures. The presence of multilayer cloud conditions in the pre-warm-frontal sector is attributed to the presence of cirrus clouds. Multilayer drizzling stratus clouds show winds veering with height, indicative of warm advection. The presence of northeasterly flow in the low levels (below 800 mbar) indicates that the ML drizzling stratus are preferentially located in the northwest quadrant of a cyclone. Multilayer nondrizzling stratus clouds have a preference to form during pre-warm-frontal conditions and southerly flow. The southerly flow clouds form in conditions that are not only warmer but also moister (r values 1.0–1.5 g kg^{-1} greater) than the other cases mainly in the lower boundary layer. In contrast, the SL drizzling and nondrizzling stratus form during post cold frontal conditions (strong northerly flow) and winds that back with height, consistent with cold air advection. Another factor that supports the preference of single-layer stratus to form under post-cold-front conditions is the lack of a low-level easterly wind component.

[26] Another parameter that we examine in correlation with the stratus cloud type is the 500 mbar vertical velocity (ω). The midlevel ω field is extracted from the ECMWF model output files. Figure 10 shows the seasonal variability of the 500 mbar ω for all four stratus clouds categories. Except for the summer months (JJA) when dynamical forcing is generally weak, SL stratus clouds (drizzling and nondrizzling) show a strong preference to form under midlevel subsidence conditions (positive ω), while ML stratus clouds prefer to form during midlevel uplifting conditions. The complete separation of single-layer and multilayer clouds into positive and negative ω regimes during the cold season is indicative of the success of the cloud type climatology to isolate distinct cloud forming regimes from cloud layering information.

6. Summary

[27] Long-term (6.5 years) ARSCL observations from the SGP ACRF in Oklahoma are used to develop a cloud climatology. The objective is to take advantage of the detailed ARSCL cloud layering information and create a cloud-type climatology based on type definitions that relate to the major dynamic and thermodynamic cloud formation processes at the SGP site. Clouds are classified with respect to cloud base

height, vertical development, and the detection of precipitation at the ground. In addition to identifying the presence of cirrus, middle, low clouds and precipitation, we developed a methodology for the separation of single-layer and multilayer cloud scenes. The retrieved parameters (hourly averaged) include cloud fraction, cloud base and cloud thickness. Boundary layer clouds were further classified with respect to their fractional coverage. In addition, continental stratus clouds were further classified into four subcategories with respect to drizzle amount and the presence or not of other cloud layers above. The classification provides a unique perspective of clouds over the ARM SGP site and aims to improve our understanding of cloud formation processes and their parameterization in large-scale models.

[28] Boundary layer clouds exhibit the strongest seasonal variability that is due to the formation of stratus associated with the presence of midlatitude frontal systems. Cirrus clouds are the most frequently observed cloud type with strong seasonal variability on cloud base height (higher cloud base during the summer months) but virtually no variability in cloud fraction. The majority of middle level clouds are thin with vertical extent below 1 km. Single-layer cloud conditions represent 23% of the total ARSCL observations. The cloud base distribution of single-layer clouds is multimodal and illustrates different levels of preference for the formation of these clouds.

[29] Multilayer cloud conditions represent a large portion (25.5%) of the observations. There does not appear to be a strong seasonal cycle in the fractional coverage of multilayer clouds. This seems surprising given the very different synoptic regimes in the winter and summer. Multilayer cloud scenes pose a problem and a challenge for satellite derived cloud climatologies. For example, multilayer cloud scenes with thin cirrus over stratus clouds can be misclassified as middle level clouds. Clear sky conditions are more frequent during the summer month (53% compared with 40% for the cold season) and precipitation is more frequent during the cold season.

[30] Overall, the stratus cloud climatology at the SGP is strongly coupled to atmospheric forcing. Stratus clouds are classified into four subcategories with respect to single-layer versus multilayer cloud fields and to the presence of drizzle. It is found that single-layer stratus situations represent about 30% of the total cloud fields and that drizzle in continental stratus appears mostly in the winter.

[31] A principal component analysis of ECMWF model output over the SGP site for the different stratus cloud classifications was performed and used to examine how the thermodynamic and wind structure varies with different cloud types. This analysis indicates that continental stratus formation is associated with strong large-scale forcing such as subsidence and advection over land. Thermodynamical composites were produced for single-layer and multilayer, and drizzling and nondrizzling stratus clouds. It was found that differences in temperature and moisture conditions separate drizzling from nondrizzling clouds while dynamic conditions separate single-layer from multilayer situations. The results illustrate that stratus clouds (drizzling and nondrizzling) show general preference to form in midlevel subsidence often associated with postfrontal conditions, but multilayer stratus clouds form preferentially during midlevel uplifting often associated with prefrontal conditions. Further, the results indicate a seasonal and potentially a thermodynamical separation between drizzling and nondrizzling low-level continental clouds.

[32] This paper presents a new ARSCL-based cloud type climatology and an application of this climatology to study dynamical influences on cloud layering and drizzle formation. The distinct dynamic and thermodynamic regimes derived for the different cloud types indicate that the cloud-type separation succeeded in isolating the major SGP cloud-forming regimes. In addition, the application of the climatology to study cloud layering and drizzle processes showed that it can be used for statistical cloud process studies that will enable us to understand the full spectrum of cloud-dynamics-thermodynamics interactions at the SGP site and to use statistical composites to evaluate model cloud simulations. A comprehensive analysis on the relationship between synoptic patterns and cloud scene types, and a comparison between the ARM sites will be the subject in future research.

[33] **Acknowledgments.** This manuscript has been authored by Brookhaven Science Associates, LLC, under contract DE-AC02-98CH1-886 with the U.S. Department of Energy. Support for this research was funded in part by the Office of Biological and Environmental Research, Environmental Sciences Division of the U.S. Department of Energy as part of the Atmospheric Radiation Measurement program.

References

Ackerman, T. P., and G. M. Stokes (2003), The Atmospheric Radiation Measurement Program, *Phys. Today*, *56*, 38–44.

Cess, R. D., et al. (1990), Intercomparison and interpretation of climate feedback processes in 19 atmospheric general circulation models, *J. Geophys. Res.*, *95*, 16,601–16,615.

Clothiaux, E. E., T. P. Ackerman, G. G. Mace, K. P. Moran, R. T. Marchand, M. A. Miller, and B. E. Martner (2000), Objective determination of cloud heights and radar reflectivities using a combination of active remote sensors at the ARM CART sites, *J. Appl. Meteorol.*, *39*, 645–665.

Del Genio, A. D., and A. B. Wolf (2000), The temperature dependence of the liquid water path of low clouds in the Southern Great Plains, *J. Clim.*, *13*, 3465–3486.

Del Genio, A. D., M.-S. Yao, W. Kovari, and K. K.-W. Lo (1996), A prognostic cloud water parameterization for global climate models, *J. Clim.*, *9*, 270–304.

Dong, X., P. Minnis, T. P. Ackerman, E. E. Clothiaux, G. G. Mace, C. N. Long, and J. C. Liljegren (2000), A 25-month database of stratus cloud properties generated from ground-based measurements at the ARM Southern Great Plains site, *J. Geophys. Res.*, *105*, 4529–4538.

Dong, X., P. Minnis, and B. Xi (2005), A climatology of midlatitude continental clouds from ARM SGP site. Part I: Low-level cloud macrophysical, microphysical and radiative properties, *J. Clim.*, *18*, 1391–1410.

Dong, X., B. Xi, and P. Minnis (2006), A climatology of midlatitude continental clouds from ARM SGP site. Part II: Cloud fraction and surface radiative forcing, *J. Clim.*, *19*, 1765–1783.

Gottschalck, J. C., B. A. Albrecht, and P. Kollias (2000), Objective synoptic classification of stratus: Impact on macroscopic cloud statistics, paper presented at 10th ARM Science Team Meeting, U.S. Dep. of Energy, San Antonio, Tex., 13–17 March.

Hahn, C. J., S. G. Warren, and J. London (1994), Edited synoptic cloud reports from ships and land stations over the globe, 1982–1991, *Tech. Rep. NDP-026B*, 47 pp., Carbon Dioxide Inf. Anal. Cent., Oak Ridge Natl. Lab., Oak Ridge, Tenn.

Harrison, E. F., P. Minnis, B. R. Barkstrom, V. Ramanathan, R. D. Cess, and G. G. Gibson (1990), Seasonal variation of cloud radiative forcing derived from the Earth radiation budget experiment, *J. Geophys. Res.*, *95*, 18,687–18,703.

Hogan, R. J., and A. J. Illingworth (2000), Deriving cloud overlap statistics from radar, *Q. J. R. Meteorol. Soc.*, *126*(569A), 2903–2909.

Hogan, R. J., C. Jakob, and A. J. Illingworth (2000), Comparison of ECMWF winter-season cloud fraction with radar derived values, *J. Appl. Meteorol.*, *40*, 513–525.

Jakob, C., R. Pincus, C. Hannay, and K.-M. Xu (2004), Use of cloud radar observations for model evaluation: A probabilistic approach, *J. Geophys. Res.*, *109*, D03202, doi:10.1029/2003JD003473.

Karl, T. R., P. D. Jones, R. W. Knight, G. Kukla, N. Plummer, V. Razuvayev, K. P. Gallo, J. Lindseay, R. J. Charison, and T. C. Peterson (1993), Asymmetric trends and daily maximum and minimum temperature, *Bull. Am. Meteorol. Soc.*, *74*, 1007–1023.

Kollias, P., and B. A. Albrecht (2000), The turbulent structure in a continental stratocumulus cloud from millimeter wavelength radar observations, *J. Atmos. Sci.*, *57*, 2417–2434.

Kollias, P., E. E. Clothiaux, B. A. Albrecht, M. A. Miller, K. P. Moran, and K. L. Johnson (2005), The Atmospheric Radiation Measurement Program cloud profiling radars. An evaluation of signal processing and sampling strategies, *J. Atmos. Oceanic Technol.*, *22*(7), 930–948, doi:10.1175/JTECH1749.1.

Lazarus, S. M., S. K. Krueger, and G. G. Mace (2000), A cloud climatology of the Southern Great Plains ARM CART, *J. Clim.*, *13*, 1762–1775.

Mace, G. G., E. E. Clothiaux, and T. P. Ackerman (2001), The composite characteristics of cirrus clouds: Bulk properties revealed by one year of continuous cloud radar data, *J. Clim.*, *14*, 2185–2203.

Moran, K. P., B. E. Martner, M. J. Post, R. A. Kropfli, D. C. Welshand, and K. B. Widener (1998), An unattended cloud-profiling radar for use in climate research, *Bull. Am. Meteorol. Soc.*, *79*, 443–455.

Morcrette, J.-J. (2002), Assessment of the ECMWF model cloudiness and surface radiation fields at the ARM SGP site, *Mon. Weather Rev.*, *130*, 257–277.

Norris, J., and C. Weaver (2001), Improved techniques for evaluating GCM cloudiness applied to the NCAR CCM3, *J. Clim.*, *14*, 2540–2550.

Ramanathan, V., R. D. Cess, E. F. Harrison, P. Minnis, B. R. Barkstrom, E. Ahmad, and D. Hartmann (1989), Cloud-radiative forcing and climate: Results from the Earth Radiation Budget Experiment, *Science*, *243*, 57–63.

Rossow, W. B., and R. A. Schiffer (1999), Advances in understanding clouds from ISCCP, *Bull. Am. Meteorol. Soc.*, *80*, 2261–2287.

Sassen, K., G. G. Mace, Z. Wang, M. R. Poellot, S. M. Sekelsky, and R. E. McIntosh (1999), Continental stratus clouds: A case study using coordinated remote sensing and aircraft measurements, *J. Atmos. Sci.*, *56*, 2345–2358.

Stephens, G. L., et al. (2002), The CLOUDSAT mission and the A-train, *Bull. Am. Meteorol. Soc.*, *83*, 1771–1790.

Stokes, G. M., and S. E. Schwartz (1994), The Atmospheric Radiation Measurement (ARM) program: Programmatic background and design of the cloud and radiation test bed, *Bull. Am. Meteorol. Soc.*, *75*, 1202–1221.

Tselioudis, G., and C. Jakob (2002), Evaluation of midlatitude cloud properties in a weather and a climate model: Dependence on dynamic regime and spatial resolution, *J. Geophys. Res.*, *107*(D24), 4781, doi:10.1029/2002JD002259.

Tselioudis, G., Y. Zhang, and W. B. Rossow (2000), Cloud and radiation variations associated with northern midlatitude low and high sea level pressure regimes, *J. Clim.*, *13*, 312–327.

Warren, S. G., C. J. Hahn, J. London, R. M. Chervin, and R. L. Jenne (1986), Global distribution of total cloud cover and cloud type amounts over land, *NCAR Tech. Note NCAR/TN-2731STR*, 231 pp., Natl. Cent. for Atmos. Res., Boulder, Colo.

Zivkovic, M., and J. Louis (1992), A new method for developing cloud specification schemes in general circulation models, *Mon. Weather Rev.*, *120*, 2928–2941.

B. A. Albrecht, Division of Meteorology and Physical Oceanography, University of Miami, Miami, FL 33149, USA.

P. Kollias, Department of Atmospheric and Oceanic Sciences, McGill University, 805 Sherbrooke Street West, Montreal, QC, Canada H3A 2K6. (pavlos.kollias@mcgill.ca)

G. Tselioudis, NASA Goddard Institute for Space Studies, New York, NY 10025, USA.